LOSS MEASUREMENTS USING A FAST TRAVERSE IN AN ILPT TRANSIENT CASCADE

by

M.L.G. OLDFIELD, D.L. SCHULTZ
Department of Engineering Science, Oxford, U.K.

and

J.H. NICHOLSON
Rolls Royce Ltd., Derby, U.K.

SUMMARY

A fast-acting downstream wake traverse has been developed to obtain turbine blade loss-coefficients in the limited 0.3 to 1.0 second running time of an Isentropic Light Piston Cascade Tunnel. The Amecke method for calculating loss coefficients is extended to cover temperature variations in the blade wake temperatures due to heat transfer to the surface of the blades. Typical results are given. Comparison of loss measurements with hot and cold flows over cold blades indicates that the normal practice of measuring losses with the blade at the flow temperature is valid.

Nomenclature

a	Sonic velocity
C_p	Specific heat
C_1	Pressure loss coefficient
C_2	Primary loss coefficient
h	Specific enthalpy
M	Mach number
$\dot{m}$	Mass flow
P	Pressure
$\dot{Q}$	Total heat transfer rate to a blade
R	Gas constant for air
R_e	Reynolds number
T	Temperature
t	Time
U	Pitchwise coordinate
V	Flow velocity
Z	Distance from blade trailing edge in axial direction
β	Relative flow angle

γ	Ratio of specific heats
η	Efficiency
θ	Critical velocity-density ratio
ρ	Density
ϕ	General flow property
Ω	Axial velocity-density ratio

Subscripts

g	Mainstream gas
0	Total conditions
s	Isentropic process
prim	Primary
ref	Reference value
1	Inlet to cascade
2	Exit of cascade, mixed out
2U	Measured by traverse at rotor exit

INTRODUCTION

In continuously running turbine blade cascade tunnels, the technique of determining aerodynamic losses by traversing a probe in the pitchwise direction behind the cascade is well established (1). Such measurements are usually made with the cascade blades at the flow temperature, it being assumed that the losses are not affected by the heat transfer to the blade which occurs in the HP turbine of an engine. The traverse speed is usually low, and hence the pressures measured are effectively time-averaged at each position of the traversing probe.

Transient cascade tunnels coupled to computer based instrumentation are cost-effective for both aerodynamic and heat transfer measurements as the energy required to drive the tunnel is low. However, there are problems associated with the high traverse speeds necessary with the short run times available.

This paper describes the use of a fast-acting traversing wake probe for measuring losses in the Oxford Isentropic Light Piston Tunnel Cascade (ILPT), and demonstrates that losses can be measured in the 0.3 to 1.0 second running time of the tunnel.

In using a fast traverse in a hot transient tunnel the following questions must be answered:

(a) Is it possible to accurately measure losses with a fast traverse?

(b) What is the effect of free stream turbulence on this measurement?

(c) As it is possible to run the ILPT hot or cold, are the cascade losses affected by heat transfer to the blade and the associated thermal gradients in the blade boundary layers?

OXFORD ILPT CASCADE

The Oxford ILPT cascade is used primarily as a heat transfer tunnel (2,3,4). It generates a flow having a stagnation temperature of 430 K ("hot") or 300 K ("cold") over a cascade of blades at 290 K. Full scale Reynolds and Mach Numbers, and flow-to-wall temperature ratios can be achieved for flow durations of between 0.3 and 1 second. A typical cascade (5) has seven passages of 44 mm chord by 50 mm span blades.

CHOICE OF DOWNSTREAM TRAVERSING PROBE

There are many factors which can influence the choice of the type of pressure probe to be used for flow measurements (1). In addition to normal requirements, pressure probes for use in a transient facility must take measurements in a relatively short time. Many of the probes suitable for loss measurements operate in the nulling mode where the probe is aligned with the flow at each measuring point. Operation in this mode is impractical with transient cascades, and it is necessary to incorporate a yaw meter into the measuring probe. The second disadvantage of many probes (which applies to their use in transient and continuous cascades) is that each pressure is measured at a different pitchwise location. The large gradients in flow properties in a wake region can cause errors in the measurement even after corrections for pitchwise displacement have been made. The requirement that the

flow parameters be measured at equal pitchwise locations prohibits the use of cone, wedge or spherical probes.

The short operating time of transient facilities dictates that the pressure transducer must be positioned as close to the sensor as possible, to give an acceptable frequency response. With certain probe designs this can significantly increase the probe dimensions and consequently its effect on the flow field.

Careful consideration of the above factors and of the environment in which the probe was to operate ($T_0 \simeq 430$ K, $P_0 \simeq 800$ kPa, $M < 1.0$) showed that the most suitable type of probe available had been successfully used by KIOCK (6). A lengthy probe development exercise was avoided by using a directly scaled down version of this "Neptune" probe.

The probe is shown in Figure 1. It consists of three hyperdermic tubing sensors to measure the flow total pressure, static pressure and direction. The static probe hyperdermic tube was constructed with an elliptical tip and cylindrical tube. The static pressure tappings were positioned 5 mm from the tip. The total probe has an inner-to-outer diameter ratio of 0.4, which is within the range of 0.3 to 0.5 recommended by the A.S.M.E. The yawmeter is constructed from two tubes fastened together with their axes in the plane of the total and static tube axes. The ends of these tubes are machined at 45° to the plane of the tube axes. This arrangement for the yawmeter allows accurate measurement of the flow angle in the presence of a pressure gradient in the traverse direction. Any influence of one sensor on another was taken into account by the probe calibration.

Each sensor is fastened to a housing containing a Kulite XCQL-093 ,100 psi, differential pressure transducer. The sensing elements are fastened to the main probe body using a removable locking plate. This arrangement allows the sensors to be interchanged with one another, or for them to be replaced by some other type of transducer, for example a thermocouple. Each Kulite transducer is powered and, amplified using Maywood differential bridge amplifiers.

The assembled probe is held on a quadrant support structure which allows independent adjustment of position and incidence angle. The support structure, although large, is mainly outside the exit flow and is shown by the schlieren photograph in Figure 2 to produce a negligible disturbance to the flowfield.

The angle of the probe is measured for each run from a schlieren photograph taken during the run, thereby minimising any error due to probe deflection during a run.

The probe and support structure are driven by an air actuated traverse mechanism. The maximum length of traverse is 100 mm.

The timing of a traverse during a typical cold tunnel run is shown in Figure 3. For this run the traverse mechanism was triggered approximately 0.3 seconds after the flow started and moved for approximately 0.45 seconds. The oscillations in the downstream total pressure follow those in upstream total pressure and the two measured wakes are clearly shown. At the end of the traverse ($t \simeq 0.8$ seconds) the Neptune probe is in a third blade wake, and the downstream total pressure remains at the low level for the remainder of the tunnel run.

The variation of flow angle and static pressure through the blade wakes is shown on their respective traverses. The rise in mean level of the downstream static pressure during the run is due to the dump tank filling.

To ensure that the reduced size Neptune probe design was suitable, a demonstration probe was built without the Kulite transducers in position. This probe was calibrated using mercury manometers in a 9" x 3" working section continuous tunnel with atmospheric inlet total conditions. These conditions gave a Reynolds number during calibration close to that at which the probe would be used. KIOCK (6) investigated the effect of varying the Reynolds number on the probe calibration and found its effect to be negligible. No variation of the Reynolds number was made in the present calibration. The calibration was made over a range of Mach numbers from 0.3 to 0.9. The probe is unsuitable for use in flow at a Mach number greater than unity.

The probe calibrations are similar to those obtained by KIOCK (6). The total probe has a negligible error over the range of Mach numbers and incidence angles of interest, whilst the static probe has an essentially constant error of 1% of the dynamic head. The yawmeter calibration is linear over a $\pm 8^{o}$ incidence range.

The calibrations were checked for the probe with pressure transducers by positioning the probe in the known mid-passage flow behind the test cascade.

DEFINITIONS OF EFFICIENCY

There are several suitable definitions of loss coefficients and efficiencies available from the literature (7,8). It is useful, however, to define the coefficients used in this paper.

Total Pressure Loss Coefficient

$$\text{Defined as } C_1 = \frac{P_{01} - P_{02}}{P_{02} - P_2} \qquad (1)$$

The stations at which the pressures are defined are shown in Figure 4.

Primary Efficiency and Loss Coefficient

$$\text{Defined as } \eta_{prim} = \frac{\text{Actual kinetic energy leaving cascade}}{\text{Ideal kinetic energy leaving cascsde}}$$

The primary efficiency is a measure of the loss of kinetic energy through the passage.

In terms of enthalpy h,

$$\eta_{prim} = \frac{h_{02} - h_2}{h_{01} - h_{2s}} \qquad (2)$$

For an ideal gas, h = CpT and for an isentropic process

$$\frac{T}{T_0} = \left(\frac{P}{P_0}\right)^{\frac{\gamma - 1}{\gamma}}, \text{ and so}$$

$$\eta_{prim} = \left(\frac{T_{02}}{T_{01}}\right) \frac{\left(1 - \left(P_2/P_{02}\right)^{\frac{\gamma - 1}{\gamma}}\right)}{\left(1 - \left(P_2/P_{01}\right)^{\frac{\gamma - 1}{\gamma}}\right)} \tag{3}$$

The Primary Loss Coefficient is defined as

$$C_2 = 1 - \eta_{prim} \tag{4}$$

ANALYSIS OF RESULTS

To calculate the performance coefficients from the traverse data taken downstream of a cascade it is necessary to calculate the values of the "mixed out" flow parameters from the pitchwise varying measured quantities. This analysis is well established in the literature and SCHIMMING and STARKEN (9) summarise the methods widely used. They point out that the approach taken by AMECKE (10) is the most correct method as it is consistent with the laws of conservation of mass, momentum and energy downstream of the cascade. The conservation equations are applied to a control volume downstream of the cascade row as shown in Figure 4. The flow at inlet to the control volume is characterised by the measured flow parameters $\phi(U)$, where $\phi = P_0$, P, β, T_0. The three conservation equations are applied to the flow through the control volume, allowing the "mixed out" uniform properties ϕ to be calculated.

It is assumed in AMECKE's analysis that the total temperature is constant at the inlet to the control volume. This is valid for equal gas: coolant:blade temperatures but not for hot mainstream gas flowing over cooler blades with an unequal coolant gas temperature. The ability of the ILPT to operate with heat transfer and unequal gas/coolant/blade temperatures requires an extension to the analysis of AMECKE. The analysis is extended below to take into account an arbitrary total temperature variation to enable an investigation of the effect of heat transfer to the blades to be made.

Consider a control volume, shown in Figure 4 with measured total pressure, total temperature, static pressure and flow angle at inlet.

The equation of continuity gives

$$\frac{1}{t} \int_0^t \rho_{2U} V_{2U} \cos\beta_{2U} dU = \rho_2 V_2 \cos\beta_2 \tag{5}$$

The momentum equation applied perpendicular to the cascade front gives

$$\frac{1}{t} \int_0^t (\rho_{2U} V_{2U}^2 \cos^2\beta_{2U} + P_{2U}) dU = \rho_2 V_2^2 \cos^2\beta_2 + P_2 \tag{6}$$

and parallel to the cascade front

$$\frac{1}{t} \int_0^t \rho_{2U} V_{2U}^2 \cos\beta_{2U} \sin\beta_{2U} dU = \rho_2 V_2^2 \cos\beta_2 \sin\beta_2 \tag{7}$$

Finally, the conservation of energy gives

$$\frac{1}{t}\int_0^t T_{02U}\rho_{2U}V_{2U}\cos\beta_{2U}dU = T_{02}\rho_2 V_2\cos\beta_2 \tag{8}$$

Equations (5) and (8) can be normalised by $\rho_{2U}{}^*a_{2U}{}^*$, the sonic conditions to yield

$$\frac{1}{t}\int_0^t \frac{P_{02U}}{P_{01}}\sqrt{\frac{T_{01}}{T_{02U}}}\,\theta_{2U}\cos\beta_{2U}dU = \frac{P_{02}}{P_{01}}\sqrt{\frac{T_{01}}{T_{02}}}\,\theta_2\cos\beta_2 \tag{9}$$

and

$$\frac{1}{t}\int_0^t \frac{T_{02U}}{T_{01}}\frac{P_{02U}}{P_{01}}\sqrt{\frac{T_{01}}{T_{02U}}}\,\theta_{2U}\cos\beta_{2U}dU = \frac{T_{02}}{T_{01}}\frac{P_{02}}{P_{01}}\sqrt{\frac{T_{01}}{T_{02}}}\,\theta_2\cos\beta_2 \tag{10}$$

where θ = critical velocity density ratio = $\frac{\rho V}{\rho^* a}$

$$\text{So}\quad \theta_{2U} = \sqrt{\frac{2}{\gamma-1}}\sqrt{\left(\frac{\gamma-1}{2}\right)^{\frac{\gamma+1}{\gamma-1}}}\left(\frac{P_{2U}}{P_{02U}}\right)^{\frac{1}{\gamma}}\sqrt{1-\left(\frac{P_{2U}}{P_{02U}}\right)^{\frac{\gamma-1}{\gamma}}} \tag{11}$$

The LHS of equations (9) and (10) can be numerically evaluated from the experimental data, to have values of I_1 and I_4 respectively. T_{02} can be calculated using equations (9) and (10) with the evaluated integrals from

$$T_{02} = \left(\frac{I_4}{I_1}\right)T_{01} \tag{12}$$

and rearranging equation (9)

$$\frac{P_{02}}{P_{01}}\,\theta_2\cos\beta_2 = I_1\sqrt{\frac{I_4}{I_1}} \tag{13}$$

Equations (6) and (7) can be normalised by the total pressure upstream of the cascade and the integrals evaluated from the experimental data:

$$\frac{P_{02}}{P_{01}}\left(\frac{\frac{1}{2}\rho_2 V_2{}^2 2\cos^2\beta_2}{P_{02}} + \frac{P_2}{P_{02}}\right) = I_2 \tag{14}$$

$$\frac{P_{02}}{P_{01}}\left(\frac{\frac{1}{2}\rho_2 V_2{}^2}{P_{02}}\cos\beta_2\sin\beta_2\right) = I_3 \tag{15}$$

where

$$I_2 = \frac{1}{t}\int_0^t \frac{P_{02U}}{P_{01}}\left(\frac{\frac{1}{2}\rho_{2U}V_{2U}{}^2}{P_{02U}}2\cos^2\beta_{2U} + \frac{P_{2U}}{P_{02U}}\right)dU \tag{16}$$

$$I_3 = \frac{1}{t} \int_0^t \frac{P_{02U}}{P_{01}} \left(\frac{\frac{1}{2}\rho_{2U} V_{2U}^2}{P_{02U}} \cos\beta_{2U} \sin\beta_{2U}\right) dU \tag{17}$$

and the relation

$$\frac{\frac{1}{2}\rho V^2}{P_0} = \frac{\gamma}{\gamma - 1} \left(\frac{P}{P_0}\right)^{\frac{1}{\gamma}} \left[1 - \left(\frac{P}{P_0}\right)^{\frac{\gamma-1}{\gamma}}\right] \tag{18}$$

is used to evaluate equation (16) and (17) with P_{01} a measured constant value.

Equations (13), (14) and (15) are of a similar form to those in AMECKE (10), and in fact reduce to identical equations when T_{02U} = constant. The solution of the equations given by AMECKE can therefore be used. So, if

$$I_0 = I_1 \left(\frac{I_4}{I_1}\right) \tag{19}$$

then

$$M_2^* = \frac{V_2}{a_2^*} = \left\{ \left(\frac{\gamma+1}{2}\right)^{\frac{2}{\gamma-1}} \left(\frac{I_2}{I_0}\right)^2 \left[\frac{1}{2} - \left(\frac{2}{\gamma+1}\right)^{\frac{2}{\gamma-1}} \left(\frac{I_0}{I_2}\right)^2 + \frac{\gamma+1}{2\gamma} \left(\frac{I_3}{I_2}\right)^2 \right] - \right.$$

$$\left. - \sqrt{\frac{1}{4} - \frac{2}{\gamma+1}^{\frac{2}{\gamma-1}} \left(\frac{I_0}{I_2}\right)^2 + \frac{\gamma^2-1}{4\gamma^2} \left(\frac{I_3}{I_2}\right)^2} \right\}^{\frac{1}{2}} \tag{20}$$

$$\frac{P_2}{P_{02}} = \left(1 - \frac{\gamma-1}{\gamma+1} M_2^{*2}\right)^{\frac{\gamma}{\gamma-1}} \tag{21}$$

$$\beta_2 = \sin^{-1} \left\{ \frac{I_3}{I_0} \quad \frac{\theta_2}{2\left(\frac{\frac{1}{2}\rho_2 V_2^2}{P_{02}}\right)} \right\} \tag{22}$$

where θ_2 and $\frac{\frac{1}{2}\rho_2 V_2^2}{P_{02}}$ are found using equations (11) and (18),

$$\frac{P_{02}}{P_{01}} = \frac{I_0}{\theta_2 \cos\beta_2} \tag{23}$$

Using equations (12), (20), (21), (22) and (23) the mixed out uniform flow properties can be calculated, and the performance coefficients established.

A check on the accuracy of the measurements can be made by calculating the axial velocity density ratio $\Omega = (\rho V)_{out}/(\rho V)_{in}$ across the cascade.

Ideally this should, of course, be unity for a two dimensional flowfield.

A comprehensive suite of computer programs were written to apply the extended AMECKE analysis and to manipulate and plot the experimental data.

EXPERIMENTAL ACCURACY

An investigation of the effect of experimental errors on the calculated loss coefficients was made.

To minimise "static" calibration errors, differential transducers were used where appropriate, and an error analysis predicted that the actual experimental errors were expected to be:

M_1	±1%	C_1	±5 - 10%
M_2	±1%	Ω	±5%

The second type of error which may occur is dynamic in nature and takes two forms. The first source of error is probe vibration or deflection which leads to an undetected error in the recording of position. This is checked by measuring the distance between two measured wakes which should equal exactly the pitch. Figure 5 shows a typical plot of total pressure loss against position. Figure 6 shows the two wakes enlarged and with the origin of the second wake displaced by one pitch. The wakes superimpose well, showing any unrecorded probe deflection is negligible.

The short measuring time of the downstream flow properties and the high system frequency response gave only a small amount of flow-property time-averaging. (The sampling rate for most of the measurements taken was 550 Hz and to prevent aliasing errors the signal from each transducer was filtered to 100 Hz). Consequently any random turbulent fluctuations of the flow will be recorded, and this can be regarded as a second possible source of dynamic error. The steady state loss is required and so it is necessary to demonstrate that random fluctuations do not affect the calculated loss. This is done using two methods: An average of the traces from many runs should produce a smooth trace since the fluctuations are random. The calculated loss is insensitive to signal noise if the value from this trace equals the average of the values from the individual runs. Six runs were averaged, each shown in Figure 7 to produce the smooth trace shown in Figure 8. The average of the losses from each individual run is 3.51% and the loss of the averaged data is 3.46%, demonstrating that the calculation procedure removes the signal noise effect.

Secondly, a random error was numerically imposed on the smooth trace shown in Figure 8. The signal shown in Figure 9 was obtained. The loss coefficient calculated from this trace was 3.49%, again demonstrating that a random signal fluctuation does not cause significant error in loss calculations.

THE EFFECT OF FREESTREAM TURBULENCE LEVEL

When a bar grid was placed upstream of the cascade to raise the upstream turbulence level from < 0.2% to 4%, it was discovered that the grid introduced slight variations in the total pressure field across the front of the cascade. This gave rise to errors in the calculated loss measurements which could only be removed by measuring P_{01} with a pitot probe stationed directly upstream of the passage being traversed.

Figures 10 and 11 show the effects of upstream turbulence on the losses of a test cascade.

EFFECT OF DIRECTION AND POSITION OF TRAVERSE

It was important to demonstrate that the direction of traverse and the position of traverse downstream of the blades did not affect the computed loss coefficients. The total pressure loss trace for an upward traverse is shown in Figure 12 and from a downward traverse is shown in Figure 13. The plots are such that the left hand wake on each corresponds to the lower blade. The loss calculated from the lower blade for upward and downward traverses are 3.6% and 3.8% respectively and 3.7% and 4.1% for the upper blade wake. This variation is within the experimental error. As well as demonstrating independence of the measurements on direction of traverse, each traverse was made at different velocities and thus independence on traverse velocity (assuming that the filtering used on each traverse speed is suitable) is shown.

The effect of the position downstream of the blades at which the traverse is taken is shown by comparing Figure 14 and Figure 15. The results shown in Figure 14 were taken with the probe "close" ($Z/C_{ax} = 0.36$) from the blade trailing edge and that in Figure 15 "far" ($Z/C_{ax} = .66$) from the trailing edge. The mixing of the wakes with distance downstream can be seen as the maximum total pressure loss decreases and the wake width increases. The derived loss coefficients for the bottom and top blade wakes are 2.2% and 2.2% respectively for the "far" traverse and 2.4% and 2.2% for the near traverse, indicating that the losses are not affected by the position of the traverse plane.

THE EFFECT OF MACH NUMBER ON LOSS

Figure 16, from (5) shows typical loss results obtained from the high speed traverse behind two blade profiles, and demonstrates the success of the technique.

EFFECT OF HEAT TRANSFER ON CASCADE LOSS

Heat transfer to the blade surface during a hot run will reduce T_{02} and hence change the primary loss coefficient C_2 given in equation (3).

If heat transfer measurements (e.g. (5)) are available for the profile, the far downstream flow total temperature T_{02} can be calculated by applying the energy equation to a control volume enclosing a blade. For typical modern turbine profiles the ratio T_{02}/T_{01} is approximately 0.995. The effect of the temperature ratio direct multiplier in equation (3) will consequently be small and will not change the loss coefficient beyond the present experimental error bounds. For the effect of heat transfer to be significant then the pressure field must change between the adiabatic and the non-adiabatic flow cases.

It has been implicitly assumed for many years that the pressure field has been equal for the two flow types, and loss measurements have been made with equal mainstream and blade temperatures. This assumption has not previously been experimentally validated in any way. With a transient cascade facility such as the ILPT, the operating temperature can be quickly and easily changed and the loss of a profile can be measured both with and without heat transfer to the blade.

The measurement of the downstream total temperature is inherently difficult because of the low response and recovery effects of total temperature thermocouples. The mixed-out far downstream total temperature, however, can be calculated from the heat transfer rate to the blade by applying an energy balance. The analysis programs described earlier can then be used iteratively to find the distribution of some guessed downstream total temperature traverse. There is only one downstream total temperature distribution which will result in both the correct mixed-out uniform temperature and mass flow, i.e. only one which will result in the correct mixed out temperature and an axial velocity-density ratio of unity.

Referring again to Figure 4, if the measured total heat transfer to the blade is $\dot{Q}$ watts, and the mass flow in kg/sec, applying an energy balance to the control volume gives

$$\dot{m}C_P T_{01} = \dot{Q} + \dot{m}C_P T_{02}$$

which can be rearranged to give

$$T_{02} = T_{01} - \frac{\dot{Q}}{\dot{m}C_P} \tag{24}$$

For a typical turbine blade cascade with an inlet flow at a total temperature of 432 K and blades at 288 K the downstream total temperature is approximately 430 K, a loss due to heat transfer of 2 K. The analysis programs were used iteratively for two shapes of wake total temperature profile, square and triangular. It was found that, because of the small temperature drop the actual shape of the wake temperature profile did not change the computed loss coefficient or axial velocity-density ratio and for subsequent hot data analysis a square wake profile similar to that shown in Figure 17 was used.

The downstream pressures and flow angle was measured for a hot flow (432 K) over the two blades in (5). The measurements were performed at an exit Mach number close to the design value and with the turbulence grid fitted. The results are compared with those obtained by operating at the same condition but with cold flow in Figure 18. Within the experimental error the data points from both profiles with hot flow lie on the curve formed by the cold flow data points. It is concluded, therefore, that loss of a cascade without film cooling is independent of heat transfer to the blades for the cascade tested.

CONCLUSIONS

It has been shown that reliable loss measurements can be obtained using a fast acting downstream traverse in a short (0.3 sec) duration hot cascade tunnel.

The AMECKE analysis has been extended to cover temperature variations due to blade heat transfer.

It has been shown that the assumption that heat transfer does not affect blade loss coefficients seems valid, lending justification to the common procedure of measuring losses in isothermal cascades.

ACKNOWLEDGEMENTS

The authors wish to thank The Ministry of Defence/P.E. and Rolls-Royce Ltd. for advice and assistance throughout the research and for permission to publish the information in this paper.

REFERENCES

1. Sieverding, C., Pressure Probe Measurements in Cascade, Modern Methods of Testing Rotating Components of Turbomachinery (Instrumentation), A.G.A.R.D. AG 207, (1975).

2. Schultz, D. L., Jones, T. V., Oldfield, M. L. G. and Daniels, L. C., A New Transient Facility for the Measurement of Heat Transfer Rates, A.G.A.R.D. CP 229, Ankara, (1977).

3. Oldfield, M. L. G., Jones, T. V. and Schultz, D. L., On-Line Computer for Transient Turbine Cascade Instrumentation, IEEE Trans. on Aerospace Electronic Systems, Vol. AES-14, No. 5, pp. 738-749, (1978).

4. Schultz, D. L., Jones, T. V., Oldfield, M. L. G. and Daniels, L. C., Transient Testing in Transonic Cascades - Aerodynamics and Heat Transfer, Proc. Symp. on Measuring Techniques in Transonic and Supersonic Flow, C.E.R.L., (1979).

5. Nicholson, J. H., Forrest, A. E., Oldfield, M. L. G. and Schultz, D. L., Heat Transfer Optimised Turbine Rotor Blades - An Experimental Study Using Transient Techniques, A.S.M.E. Paper 82-GT-304, (1982).

6. Kiock, R., Description of a Probe for Measurements of Two-Dimensional Wake Flow Quantities, D.F.V.L.R. Braunschweig, IB1 51-74/2, (1974).

7. Dixon, S. L., Thermodynamics of Turbomachinery, Pergamon Press, (1975).

8. Horlock, ., Axial Flow Turbines, Krieger, (1973).

9. Schimming, P. and Starken, H., Data Reduction of Two-Dimensional Cascade Measurements, Modern Methods of Testing Rotating Components of Turbomachinery (Instrumentation), A.G.A.R.D. AG 207, (1975).

10. Amecke, J., Anwendung der Transsonichen "Ähnlichkietsregel auf die Stromung durchebene Schaufelgitter", Göttingen, (1968).

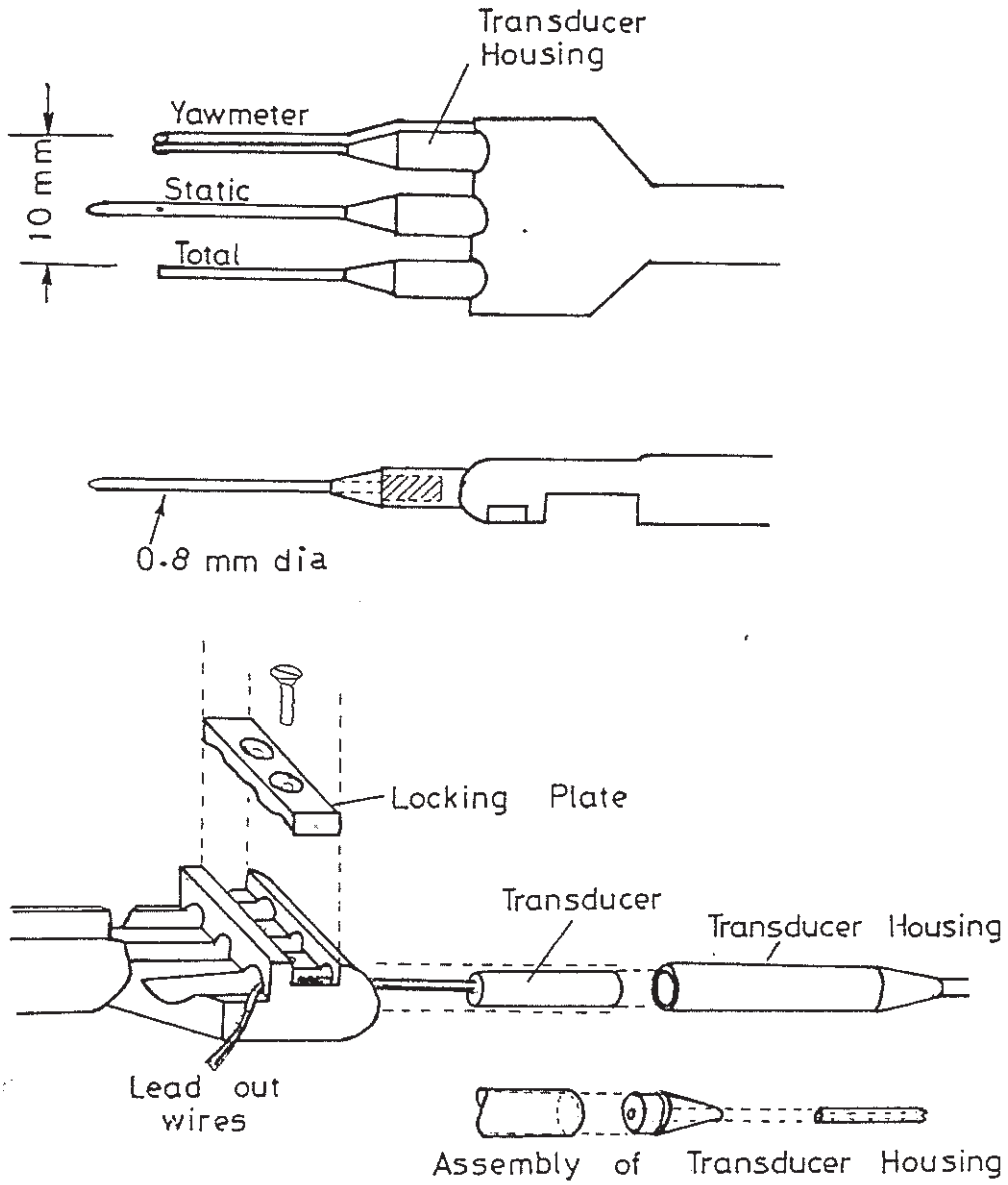

Figure 1 Neptune probe for cascade loss measurements.

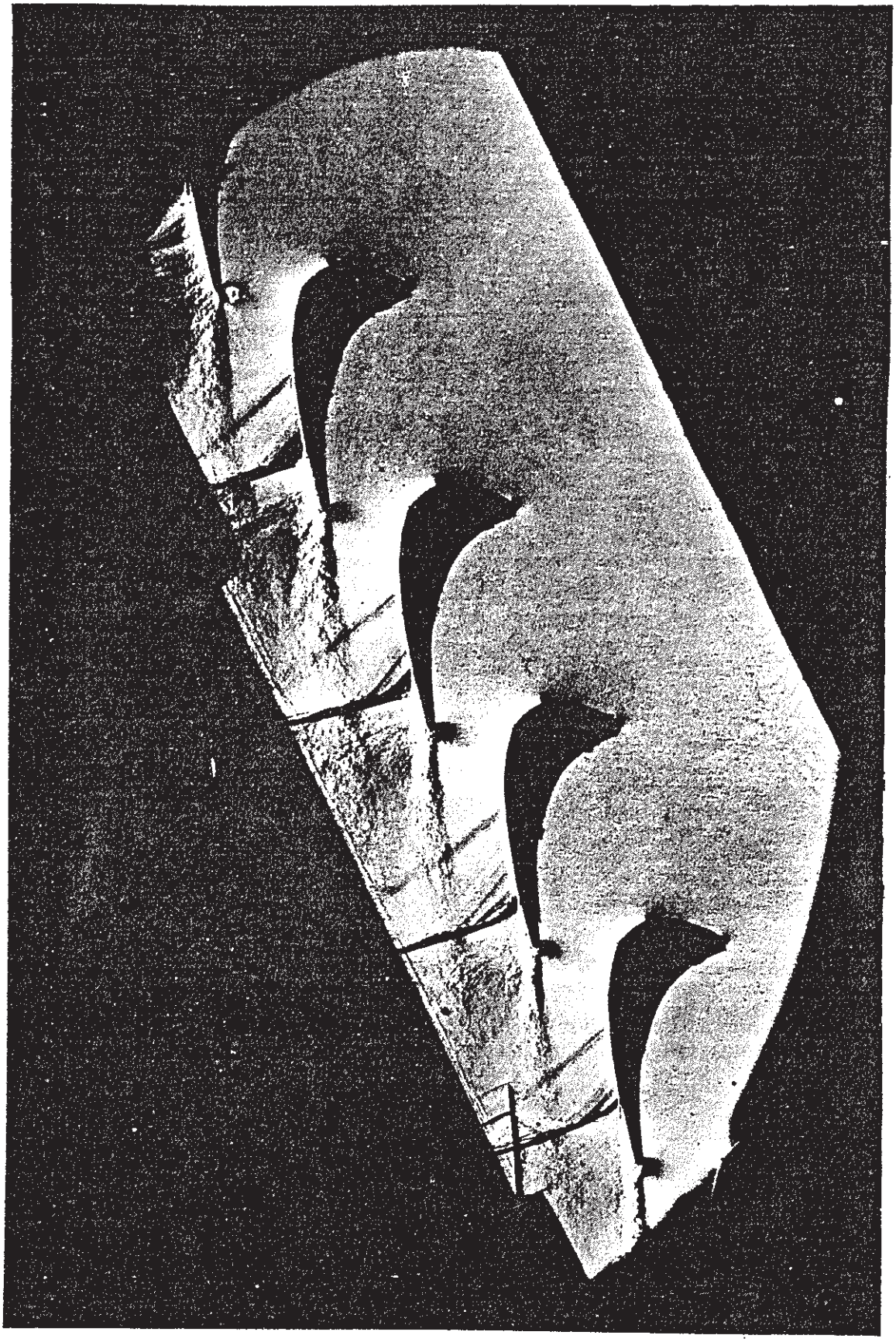

Figure 2 Typical schlieren photograph showing probe in motion (from (5)) Note lack of probe interference.

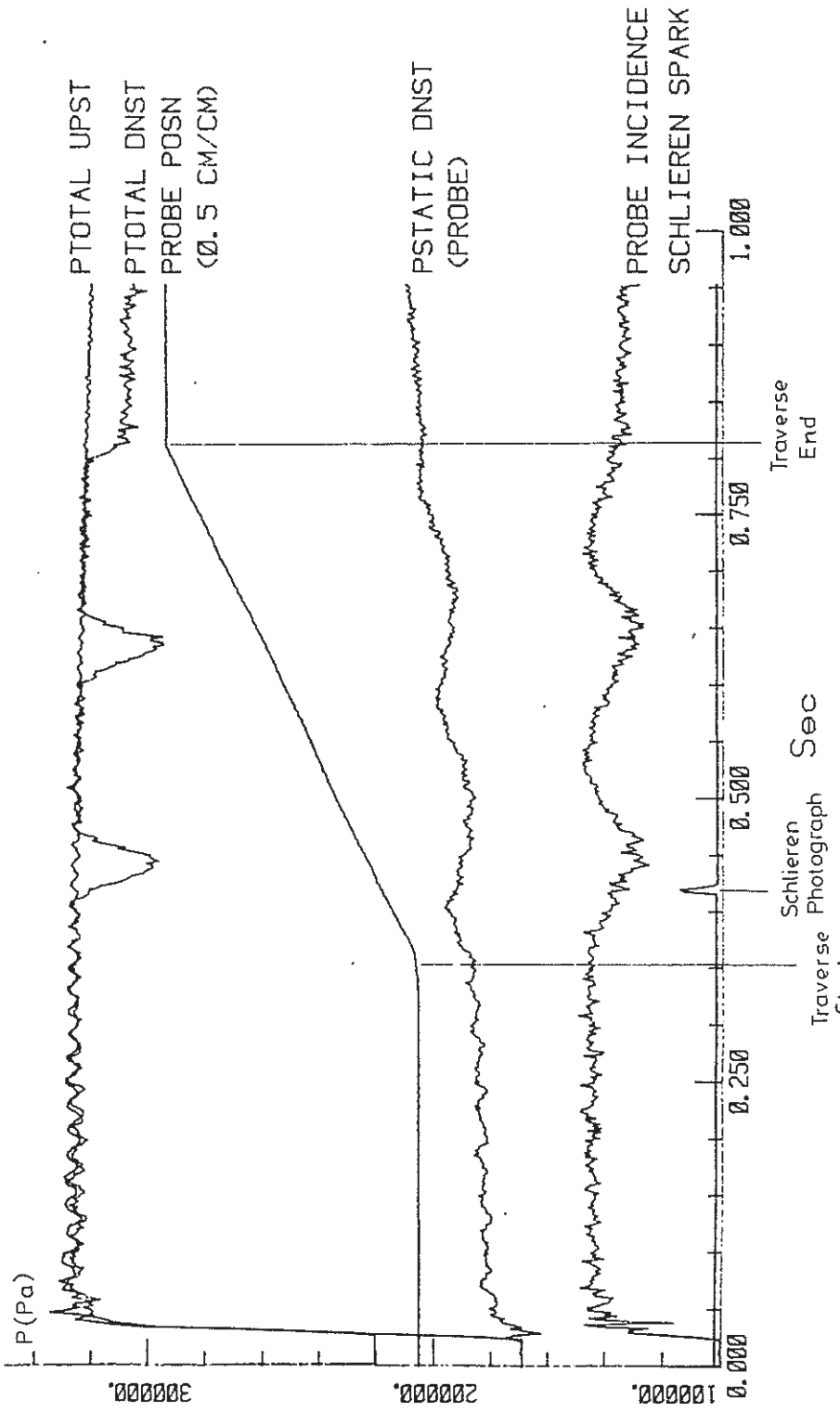

Figure 3 Downstream traverse timing during tunnel run.

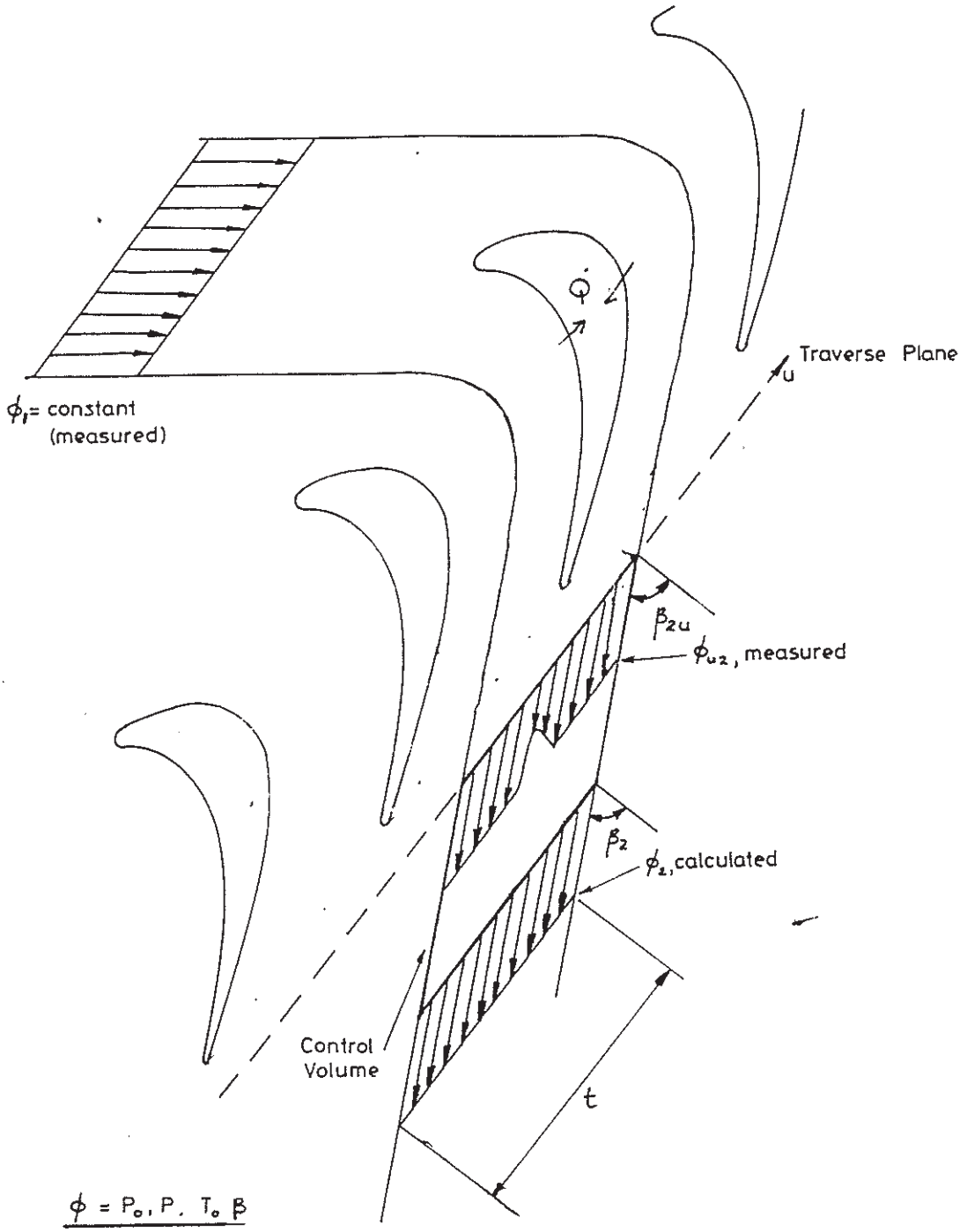

Figure 4 Downstream traverse control volume for analysis.

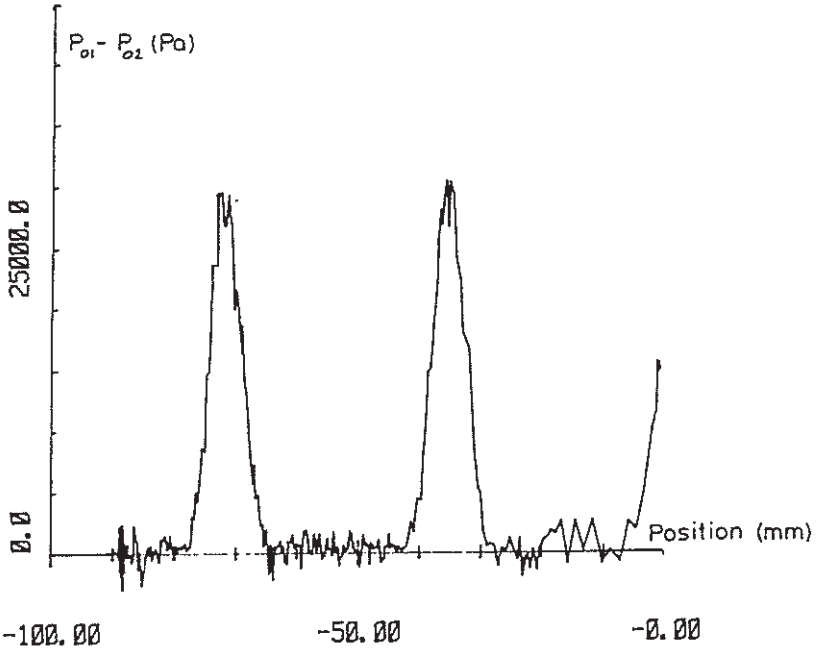

Figure 5 Typical downstream total pressure traverse.

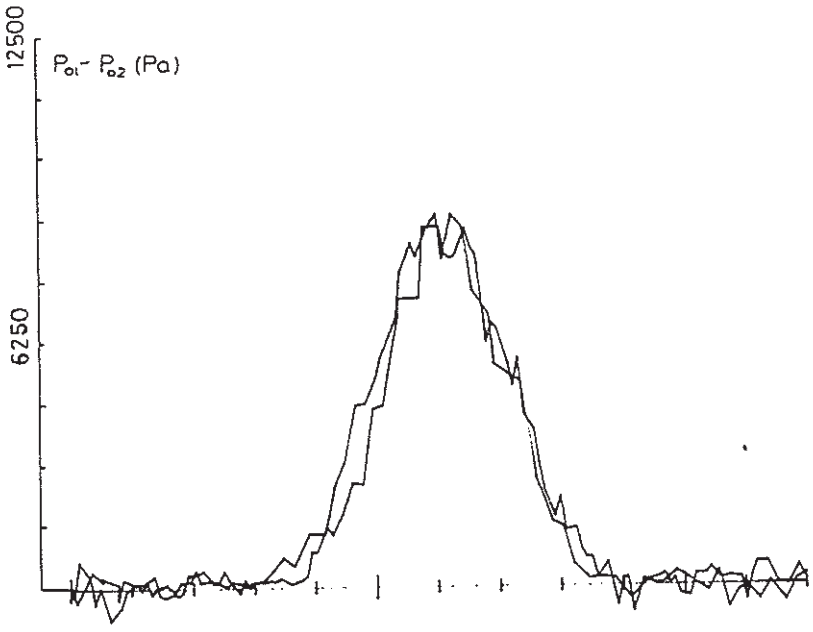

Figure 6 Downstream total pressure traverse repeatability, second wake from Figure 5 displaced by one pitch.

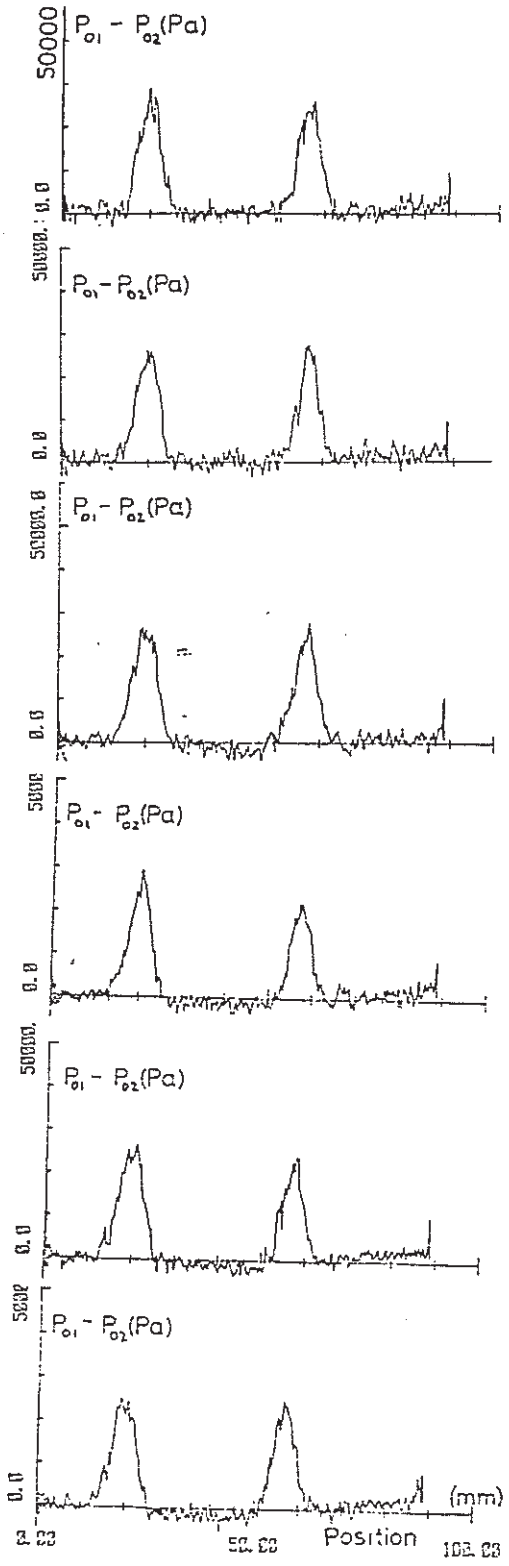

Figure 7 Six downstream pressure traverses showing random signal noise. Average loss = 3.51%.

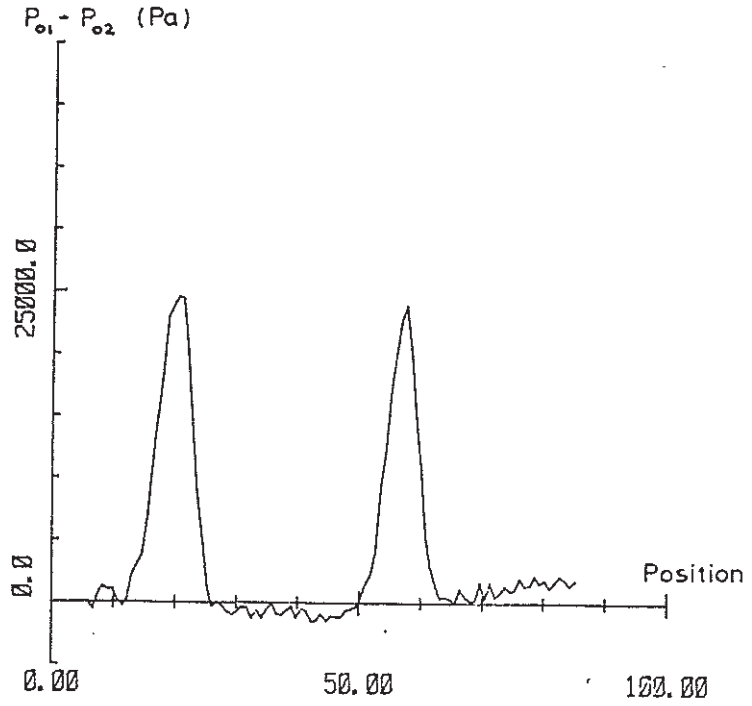

Figure 8 Smooth total pressure trace obtained by averaging six runs. Loss = 3.46%.

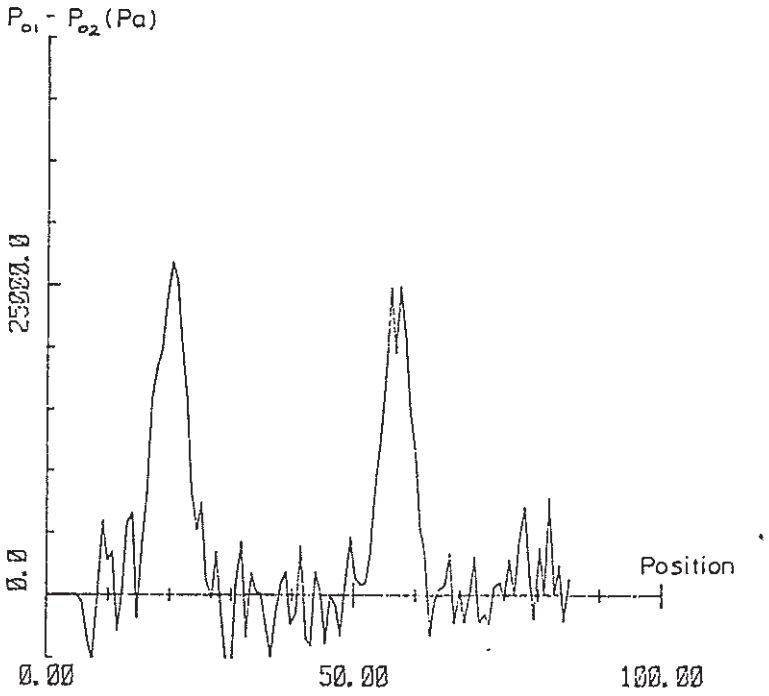

Figure 9 Numerically added random noise on curve in Figure 8. Loss = 3.49%.

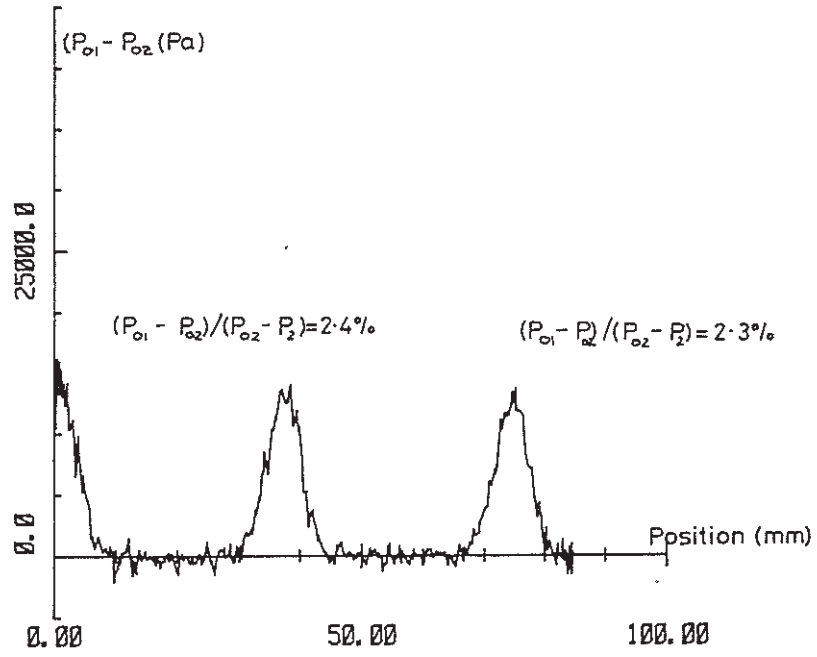

Figure 10 Downstream total pressure traverse with no turbulence grid upstream.

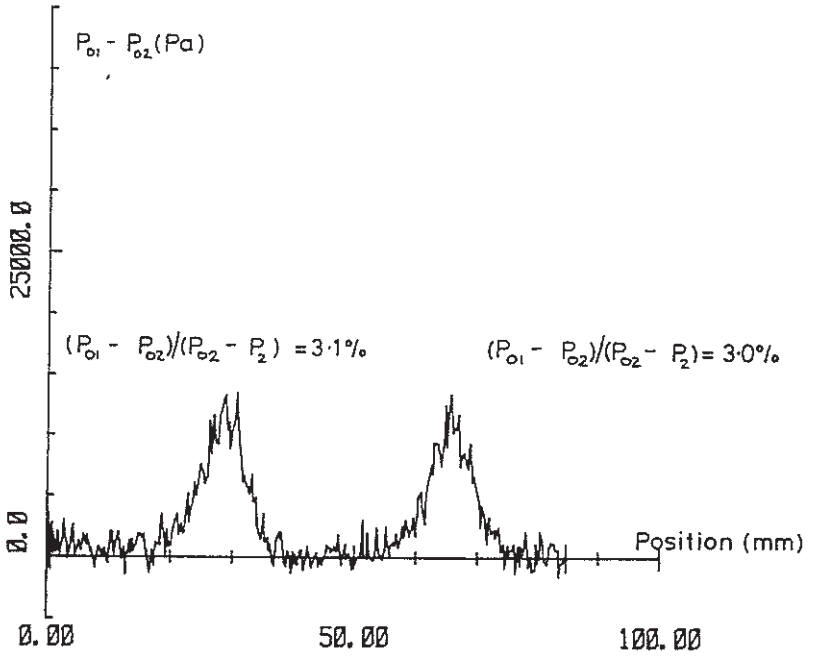

Figure 11 Downstream total pressure traverse with 4% upstream turbulence from grid and centre passage upstream total pressure measurement.

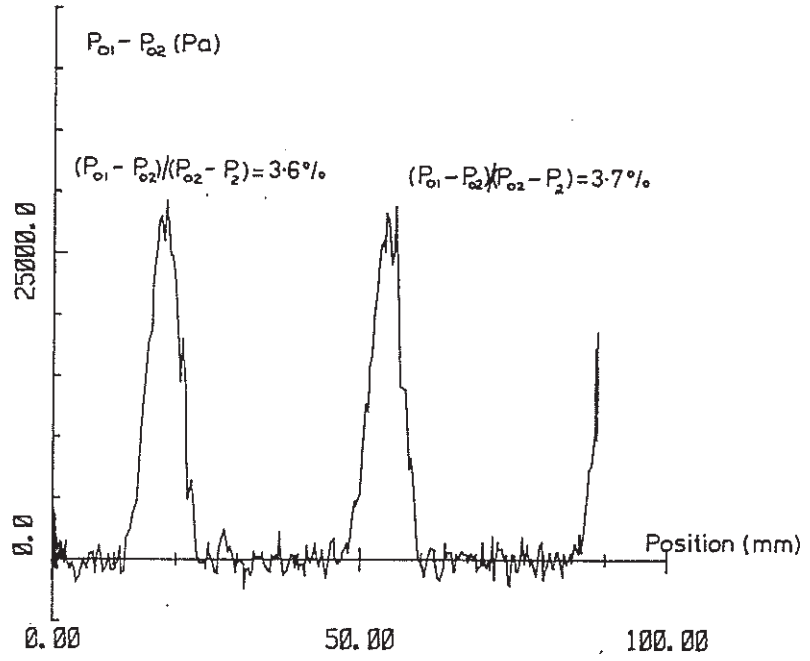

Figure 12 Downstream total pressure traverse, traverse direction positive ("upwards").

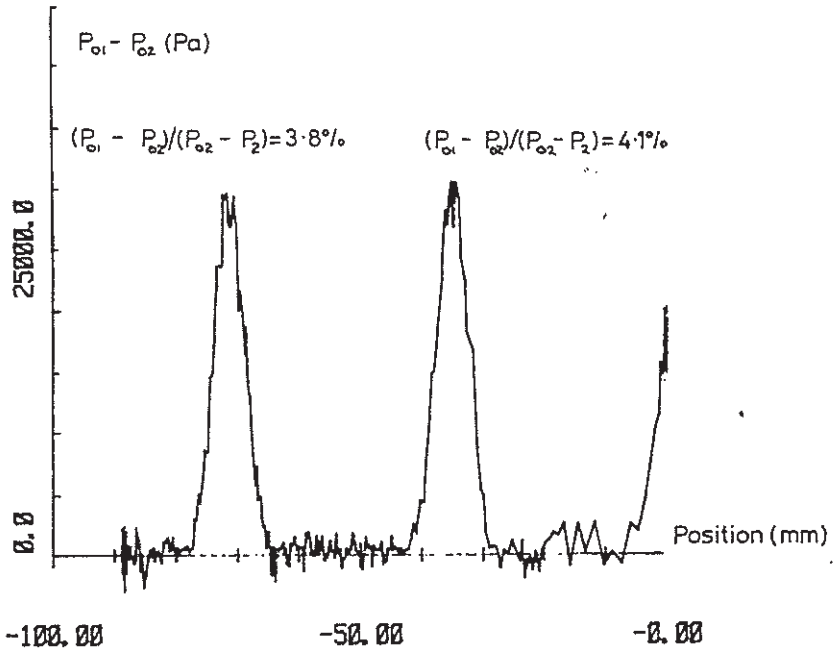

Figure 13 Downstream total pressure traverse, traverse direction negative ("downwards").

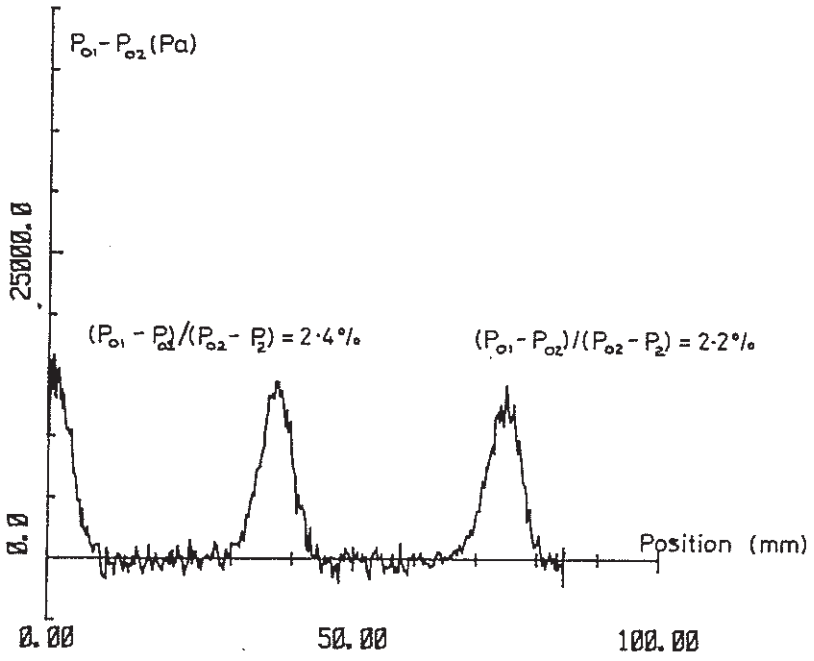

Figure 14 Downstream total pressure traverse with probe "close" (Z/Cax = 0.36).

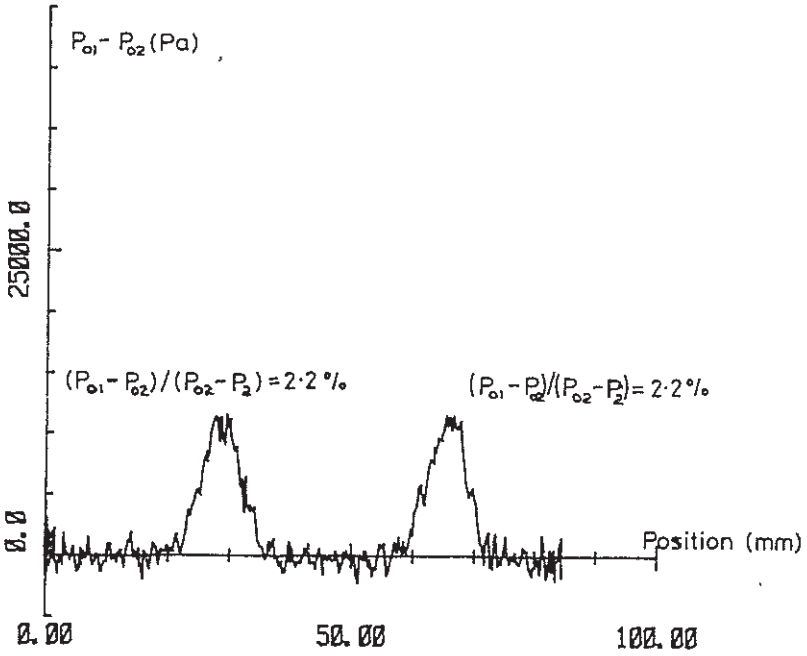

Figure 15 Downstream total pressure traverse with probe "far" (Z/Cax = 0.66).

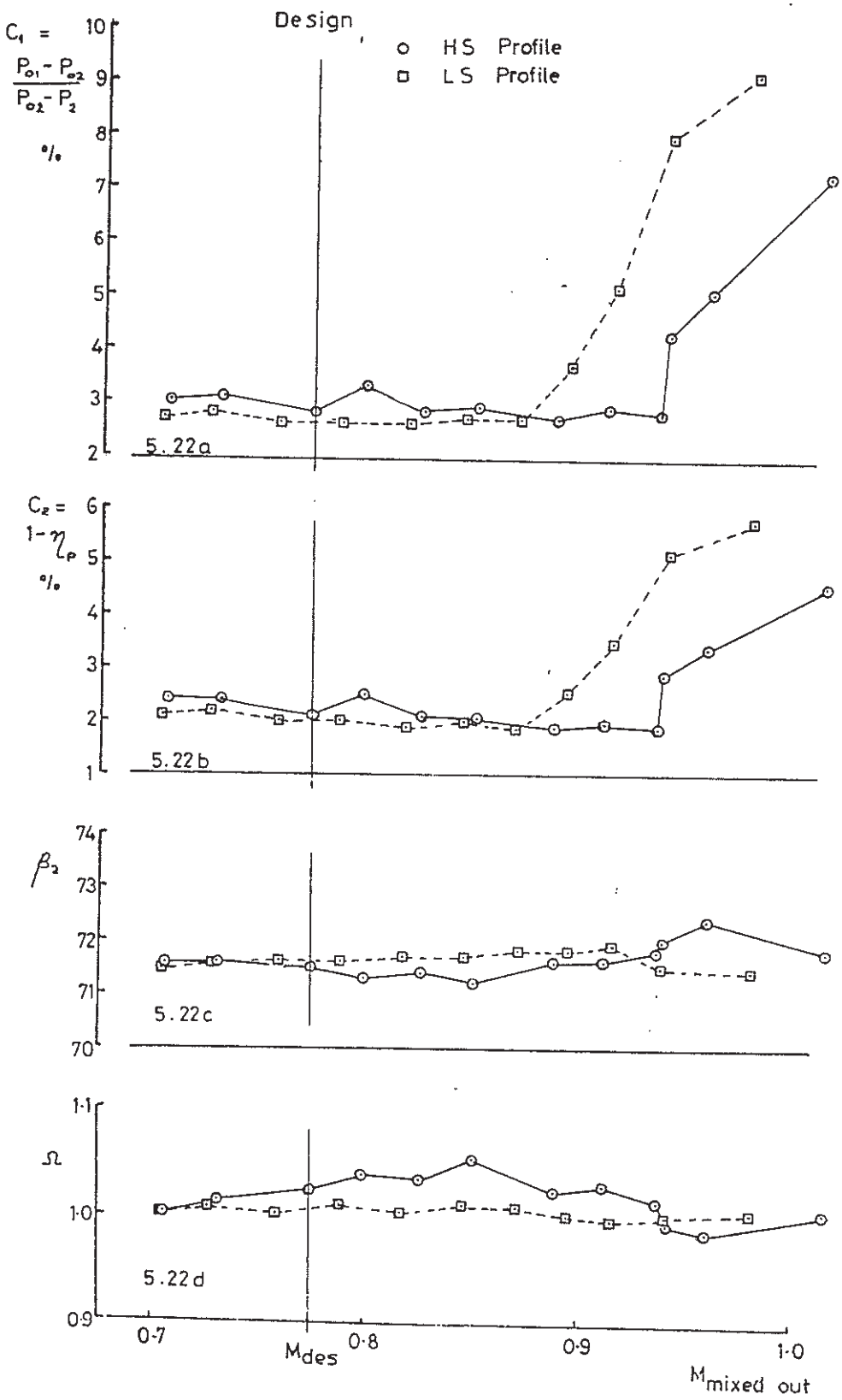

Figure 16 Profile loss data taken with fast traverse in ILPT (from (5)).

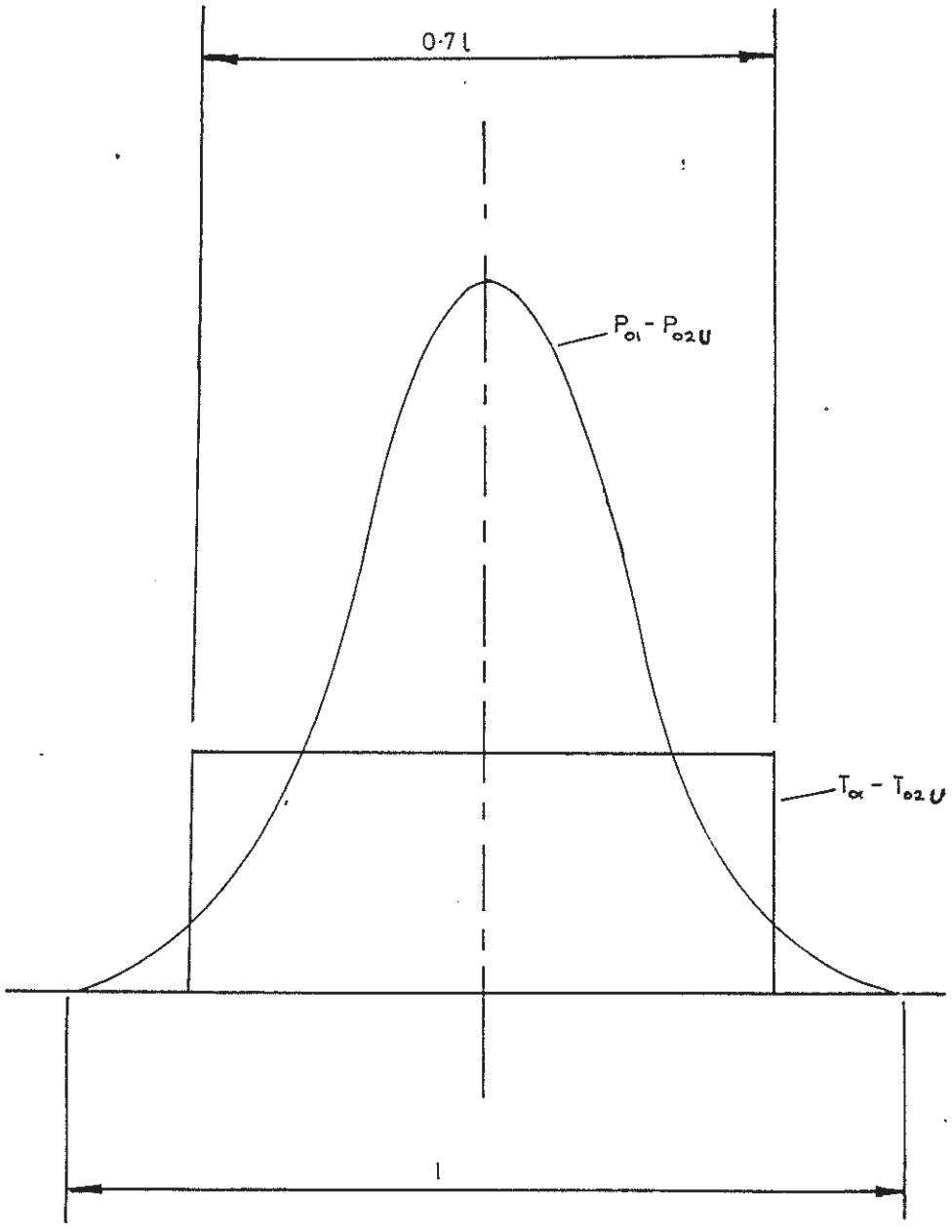

Figure 17 Square wake total temperature profile.

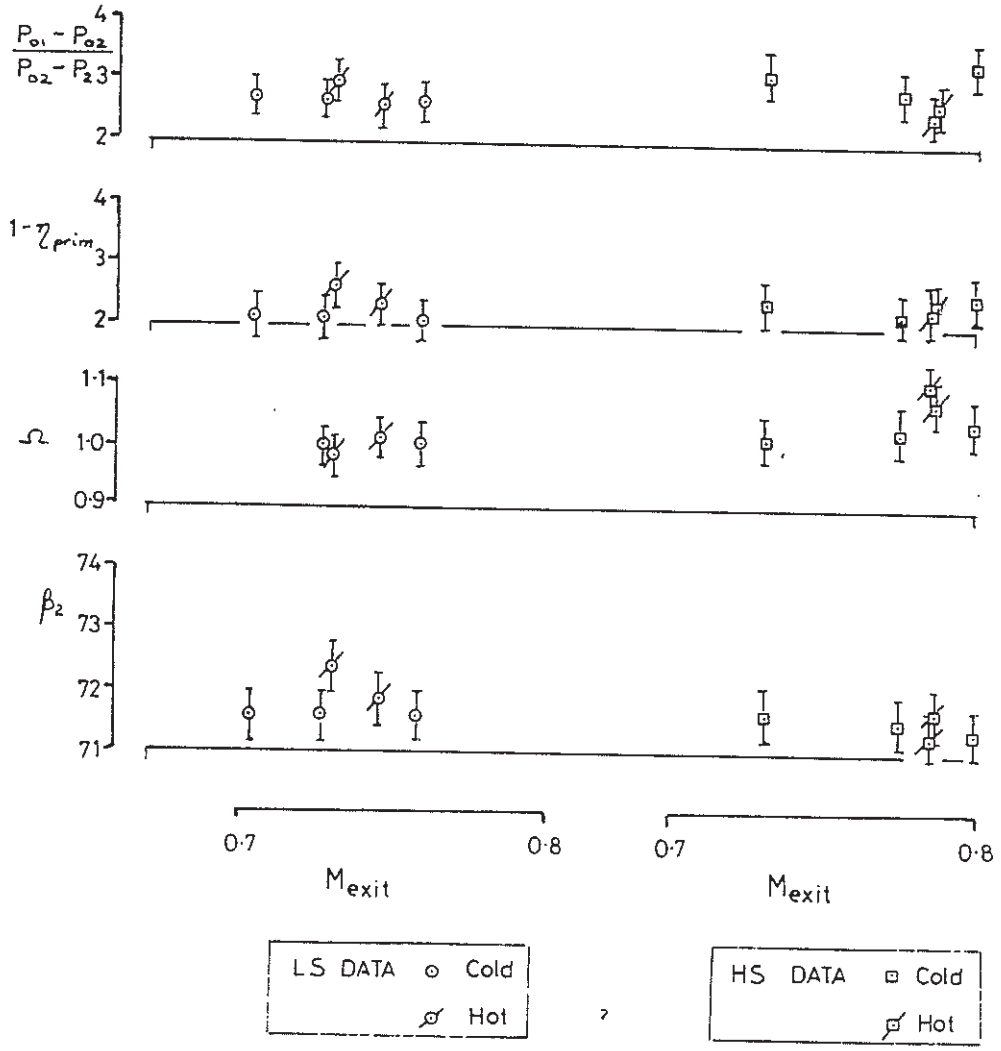

Figure 18 The effect of heat transfer on loss coefficients (from (5)).